ISBN: 978-3-95450-219-6 ISSN: 2226-0366 doi: 10.18429/JACoW-LINAC2024-THPB053

PERFORMANCE OF THE SUPER-CONDUCTING RIKEN HEAVY-ION LINAC AT THE RIKEN RADIOACTIVE ISOTOPE BEAM FACTORY

N. Sakamoto*, O. Kamigaito, K. Ozeki, K. Suda, K. Yamada, T. Nagatomo,
T. Nishi, Y. Higurashi, A. Uchiyama, RIKEN Nishina Center, Saitama, Japan

Abstract

The RIKEN superconducting heavy-ion linear accelerator (SRILAC) has been steadily supplying beams for super-heavy element synthesis experiments since its commission in January 2020 by addressing relevant issues. The decrease in the available acceleration voltage due to the increase in X-rays i.e. field emission (FE) from superconducting (SC) cavities has been a major issue. However, this issue has been mitigated via high-RF power processing (HPP). This presentation reports on the current performance of SRILAC and its prospects.

INTRODUCTION

The mission of the RIKEN Radioactive Isotope Beam Factory (RIBF [1]) in Japan is to improve our understanding of the element synthesis mechanism via experiments using intense heavy-ion beams.

In 2016, the RIKEN Nishina Center (RNC) started a comprehensive super-heavy element (SHE) research program. The main objective was to expand the periodic table of elements by synthesizing new super-heavy elements. After the discovery of oganesson (Og, Z = 118), the aim of the SHE project was to discover elements beyond Z = 118. To synthesize the Z = 119 element, the RNC adopted a combination of ^{51}V as the beam and ^{248}Cm as the target [2]. For this experiment, a beam energy of ^{51}V = 6 MeV/u with an intensity of 2.5 pμA is required. Thus, the primary focus of this project was to upgrade the accelerator by introducing a SC linear accelerator to increase the final beam energy from 5.5 to 6.5 MeV/u and a SC electron-cyclotron-resonance ion source (SC-ECRIS) to multiply its beam intensity by a factor of five (see Fig. 1).

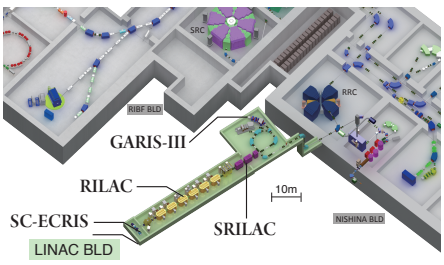

Figure 1: Birds-eye view of the RILAC.

In 2020, beam commissioning for SRILAC was successfully conducted [3], with user beam service subsequently starting [4]. Ar and V beams are provided for the experiment with an energy ranging between 4.2 and 6.3 MeV/u. Owing to the newly constructed SC-ECRIS [5] and the improvement in the RILAC transmission efficiency [6], the maximum beam intensity of 5.2 pμA (duty 100%) exceeded the project's primary target intensity. In this report, an overview and operation status of SRILAC and its relevant issues are presented. Additionally, FE and vacuum leakage from input couplers are described.

SRILAC OVERVIEW

The SRILAC layout is illustrated in Fig. 2. SRILAC comprises three cryomodules (CM1, CM2, and CM3) and a medium-energy beam-transport line (V00, V10, V20, and V30) that connects the CMs, RILAC DTLs, and a high-energy beam-transport line. As shown in Fig. 2, CM1 and CM2 contain four SC-QWRs, whereas CM3 contains only two SC-QWRs. Each SC-QWRs are labeled SC01–SC10 from upstream to downstream. The SC-QWR specifications are listed in Table 1. The operating temperature was 4.5 K. The SC-QWRs were fabricated from highly purified Nb sheets with an RRR of 250. The inner surfaces were treated using a standard processing method as follows: (i) bulk etching via buffered chemical polishing (BCP); (ii) annealing (750 °C, 3 h) in a vacuum furnace; (iii) light etching via BCP; (iv) high-pressure rinsing (HPR) with ultrapure water; and (v) baking (120 °C, 48 h). All SC-QWRs achieved the target Q_0 1×10^9 with E_{acc} = 6.8 MV/m in the acceptance tests [7]. The operating frequency of the SC-QWRs was 73 MHz. The amplitude and phase of the accelerating field could be set independently for each SC-QWR. The independent RF system for each SC-QWR enables the seamless tuning of the energy of the accelerated beams. The gap length was optimized for β = 0.078.

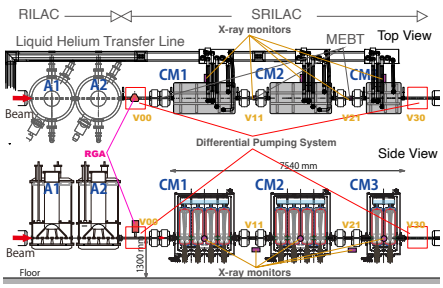

Figure 2: SRILAC layout.

One of the most crucial issues in beam-transport-line design is preventing SC cavity contamination by dust transported from the room-temperature (RT) section through gas flow owing to the vacuum pressure gradient. While the vacuum pressure level of the SC part decreases to as low as

* nsakamot@ribf.riken.jp

ISBN: 978-3-95450-219-6 ISSN: 2226-0366 doi: 10.18429/JACoW-LINAC2024-THPB053

Table 1: SRILAC Design Parameters

Parameter	
Frequency (MHz)	73.0 (CW)
E_{inj} (MeV/u)	3.6
E_{out} (MeV/u)	6.5
β_{opt}	0.078
R_{sh}/Q_0 (Ω)	579
G	22.4
E_{acc} (MV/m)	6.8
$E_{\mathrm{peak}}/E_{\mathrm{acc}}$	6.2
$B_{\mathrm{peak}}/E_{\mathrm{acc}}$ (mT/(MV/m))	9.6
Operating temperature (K)	4.5
$\Delta f/\Delta P_{\mathrm{He}}$ (Hz/hPa)	–2.0 [8]
Target Q_0	1×10^9
Q_{ext}	1–4.5×10^6

1×10^{-8} Pa, the vacuum pressure in RILAC, which was designed and built more than 40 years ago (first beam in 1981), is approximately 1×10^{-5} Pa. To connect different vacuum-level sections and prevent gas flow into the high-vacuum section, a non-evaporable getter-based differential pumping system (DPS) was developed [9]. The DPS-sandwiched CMs reduce the pressure from the vacuum of the existing RILAC beamline to the SRILAC ultra-high vacuum.

X-ray levels due to FE from the SC-QWRs are routinely measured as a function of gap voltage and continuously measured during user beam service by an X-ray monitor located at the middle of the side wall of the CM, as indicated in Fig. 2. Whereas a beam loss monitor, such as an ion chamber, has little sensitivity to the beam loss of low-energy beams, X-ray monitors are found to have some sensitivity. Two X-ray monitors were added to MEBT sections, V11 and V21, to detect beam losses where the transverse beam size reached a maximum. Because the harmful effect of a strong FE on the performance of SC-QWRs is unclear, the SRILAC operates with gap voltages below the onset gap voltage $V_{\mathrm{gap}}^{\mathrm{onset}}$ (here, $V_{\mathrm{gap}}^{\mathrm{onset}}$ is defined as the gap voltage at a 1-μSv/h X-ray monitor level). Furthermore, beam losses can be detected with a low background.

Even with countermeasures to prevent cavity performance degradation, SRILAC encountered a sudden increase in X-ray levels, and $V_{\mathrm{gap}}^{\mathrm{onset}}$ became increasingly lower. To mitigate FE, we adopted HPP to obtain the gap voltages required for acceleration [10].

OPERATIONAL HISTORY

The operational history since the first beam-acceleration test, which was performed at the end of January 2020, is shown in Fig. 3. In the figure, the blue and orange blocks indicate the duration of CM cooling to 4 K and beam operation, respectively. The yellow blocks represent regular breaks for the annual maintenance of the helium refrigerator system. In 2024, as shown in the figure, the user beam service operated continuously until April. In April 2024, the GARIS-III spectrometer was seriously damaged; therefore, the entire accelerator system was immediately shut down. Recovery from this problem is on-going, and beam service is planned to restart in October.

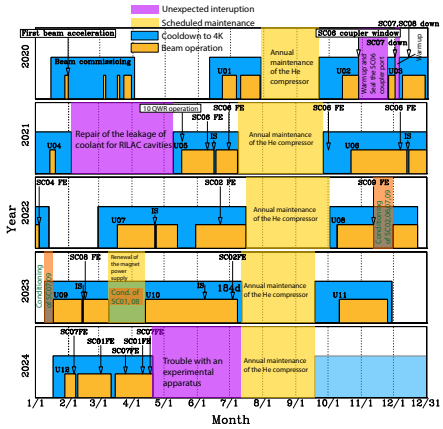

Figure 3: SRILAC operational history.

For RILAC and SRILAC, we experienced two unexpected interruptions owing to unforeseen circumstances. The first interruption was caused by a vacuum issue in CM2. In November 2019, during the initial cooling test, the vacuum leaked to the CM2 SC-QWRs. This was due to problems with the SC05 input coupler. To mitigate vacuum leakage, vacuum pumping was performed outside the input coupler. One year later, in October 2020, the CM2 vacuum level suddenly deteriorated again owing to malfunction of the SC06 coupler window. Subsequently, the beam supply was aborted. Although the beam supply was restarted, excluding SC05 and SC06, serious problems were encountered in SC07 and SC08. In fact, the gap voltages of these cavities often drop to very low levels, resulting in multipacting (MP) and an inability to maintain the acceleration voltages. We attempted to recover the cavity performance by increasing the temperature; however, this was unsuccessful. The second interruption was caused by a malfunction in the RILAC cavities in the first half of 2021. During repair, which required four months, outer vacuum windows were adopted for all coupler ports in the ten SC-QWRs to protect the coupler windows (Fig. 4). By May 2021, their operation had been successfully restored [3].

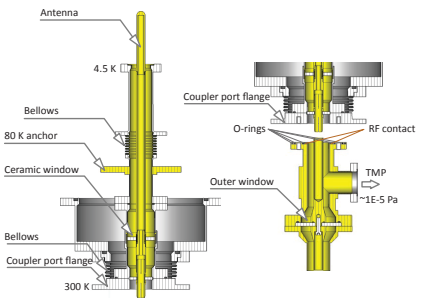

Figure 4: Schematic of the input coupler and outer window.

ISBN: 978-3-95450-219-6 ISSN: 2226-0366 doi: 10.18429/JACoW-LINAC2024-THPB053

As described above, the SC-QWRs experience continuous degradation after the issue with the SC06 coupler window [10]. A gradual increase in the X-ray levels was observed during high-power tests performed routinely after cool-down from RT; however, the increase was not serious to continue the operation. We repeatedly encountered sudden increases in the X-ray levels, which were continuously measured for each CM during beam service [10]. In November 2022, HPP was performed for the first time to mitigate the FE, which was found to work well. Details are presented in the next section.

FIELD EMISSION

We repeatedly encountered sudden increases in X-rays from the SC-QWRs during beam supply. In some cases, heavy MP were present, and the X-ray level increased after re-energizing the SC-QWRs. SRILAC operates at gap voltages below $V_{\mathrm{gap}}^{\mathrm{onset}}$. This implies that the margin of the total acceleration voltage is lost year-by-year.

To overcome this problem, we implemented HPP [11]. HPP is a traditional technology for mitigating the FE of SC cavities, and its successful processing has been previously reported [12]. For SRILAC, input pulses were produced using the amplitude modulation mode of the signal generator (SG). The amplitude modulation was set to 0.5 Hz and a 1% duty RF pulse with a 20-ms width was adopted. The 20-ms pulse width was sufficient to raise the cavity voltage to 90% with a detuning of 50 Hz, as shown in Fig. 5. The RF frequency was tuned manually to keep on resonance. The RF power was gradually increased step-by-step by observing the RF signals at P_{SG}, P_{in}, P_{ref}, P_t, vacuum, and X-ray levels. Finally, $V_{\mathrm{gap}}^{\mathrm{onset}}$ improved according to the RF power reached.

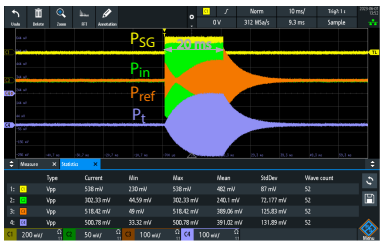

Figure 5: RF signals observed during the pulsed RF power conditioning. P_{SG}, P_{in}, P_{ref}, and P_t are the input pulse from SG, the forward signal from the directional coupler, the reflected signal, and the signal from the cavity pickup, respectively.

HPP has been adopted for online cryomodules and succeeded in reducing X-ray levels. Every single trial succeeded in reducing the FE at a given field level, and $V_{\mathrm{gap}}^{\mathrm{onset}}$ was improved. We observed that the higher RF power reached during HPP, the higher $V_{\mathrm{gap}}^{\mathrm{onset}}$ obtained. It was found that conditioning for longer times at the same field level or with longer pulses at the same field level did not reduce FEs. Some of these trials were accompanied by discharge or outgassing, after which the FE levels decreased suddenly. This succeeded even with no processing "event," such as a spark or a discharge inside the cavity; continuous RF pulse excitation mitigated the FE levels.

The X-ray levels measured before user beam service stated from January 2024 (Campaign 12) are shown in Fig. 6. At the beginning $V_{\mathrm{gap}}^{\mathrm{onset}}$ for SC03, SC05, and SC06 were as low as 1.0, 0.6, and 0.8 MV, respectively. Then HPP was performed on SC03, SC05, and SC06. The peak processing RF power for SC03, SC05, and SC06 reached 3.0, 1.7, and 2.2 MV, respectively. Subsequently, $V_{\mathrm{gap}}^{\mathrm{onset}}$ improved to 1.5, 1.0, and 1.2 MV, respectively. Currently, $V_{\mathrm{gap}}^{\mathrm{onset}}$ has been improved compared with that of the initial installation, resulting in the recovery of the available acceleration voltage. During user beam service Campaign 11 in 2023, there were no critical issues with FE. However, during Campaign 12 in 2024, FE was repeatedly observed in SC01 and SC07. We plan to investigate this phenomenon before Campaign 13, which is scheduled for October 2024.

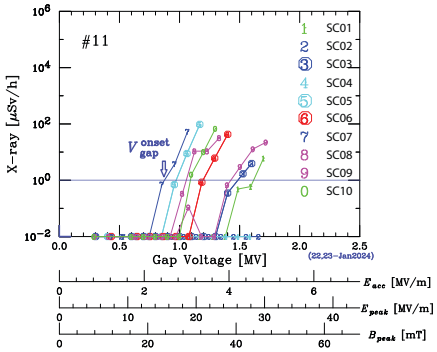

Figure 6: X-ray levels as a function of gap voltage. Each plotted number represents the SC-QWR ID. Circled plots were obtained after HPP.

Higher RF power processing is promising for improving $V_{\mathrm{gap}}^{\mathrm{onset}}$. However, it is crucial to recover damaged couplers to accept a higher RF power. The design of the coupler exchange system is underway.

CONCLUSIONS

User beam service for experiments on super-heavy element synthesis have been continuously performed since beam commissioning began in 2020. SC-QWRs suffer from sudden increases in FE during beam service. HPP was found to be effective in irreversibly reducing FE at a given field level. However, caution must be exercised to avoid critical damage due to surface crater formation. Finally, the recovery of damaged couplers is crucial for improving the cavity performance.

REFERENCES

[1] H. Okuno *et al.*, "Progress of RIBF Accelerators", *Prog. Theor. Exp. Phys.*, vol. 2012, no, 1, p. 03C002, 2012. doi:10.1093/ptep/pts046

ISBN: 978-3-95450-219-6 ISSN: 2226-0366 doi: 10.18429/JACoW-LINAC2024-THPB053

[2] H. Sakai *et al.*, "Facility Upgrade for Superheavy-Element Research at RIKEN", *Eur. Phys. J. A*, vol. 58, p.238, 2022. doi:10.1140/epja/s10050-022-00888-3

[3] K. Yamada *et al.*, "Successful Beam Commissioning of Heavy-Ion Superconducting Linac at RIKEN", in *Proc. SRF'21*, East Lansing, MI, USA, Jun.-Jul. 2021, pp. 167–174. doi:10.18429/JACoW-SRF2021-MOOFAV01

[4] K. Yamada *et al.*, "Operational Experience for RIKEN Superconducting Linear Accelerator", in *Proc. SRF'23*, Grand Rapids, MI, USA, Jun. 2023, paper MOIXA04, pp. 30–37. doi:10.18429/JACoW-SRF2023-MOIXA04

[5] T. Nagatomo *et al.*, "High intensity vanadium beam for synthesis of new superheavy elements with well-controlled emittance by using 'slit triplet'", *Rev. Sci. Instrum.*, vol. 91, p. 023318, 2020. doi:10.1063/1.5130431

[6] T. Nishi *et al.*, "Improvement of the transmission efficiency of RILAC", in *RIKEN Accel. Prog. Rep.*, vol. 55, p. 62, 2022. https://www.nishina.riken.jp/researcher/APR/APR055/pdf/62.pdf

[7] N. Sakamoto *et al.*, "Construction Status of the Superconducting Linac at RIKEN RIBF", in *Proc. LINAC'18*, Beijing, China, Sep. 2018, pp. 620–625. doi:10.18429/JACoW-LINAC2018-WE2A03

[8] K. Suda *et al.*, "New Frequency-Tuning System and Digital LLRF for Stable and Reliable Operation of SRILAC", in *Proc. SRF'21*, East Lansing, MI, USA, Jun.-Jul. 2021, pp. 666–670. doi:10.18429/JACoW-SRF2021-WEPTEV013

[9] H. Imao *et al.*, "Non-Evaporative Getter-Based Differential Pumping System for SRILAC at RIBF", in *Proc. SRF'19*, Dresden, Germany, Jun.-Jul. 2019, pp. 419–423. doi:10.18429/JACoW-SRF2019-TUP013

[10] N. Sakamoto, O. Kamigaito, K. Ozeki, K. Suda, and K. Yamada, "Degradation and Recovery of Cavity Performance in SRILAC Cryomodules at RIBF", in *Proc. SRF'23*, Grand Rapids, MI, USA, Jun. 2023, paper WEPWB085, pp. 784–789. doi:10.18429/JACoW-SRF2023-WEPWB085

[11] H. Padamsee *et al.*, "RF Field Emission in Superconducting Cavities", in *Proc. SRF'87*, Lemont, IL, USA, Sep. 1987, paper SRF87C03, pp. 251–272.

[12] E. Kako *et al.*, "Degradation and Recovery of Cavity Performances in Compact-ERL Injector Cryomodule", in *Proc. SRF'17*, Lanzhou, China, Jul. 2017, pp. 289–293. doi:10.18429/JACoW-SRF2017-MOPB097